CrossMark

ORIGINAL ARTICLE

Groundwater trace element chemistry of the karstified limestone of Andhra Pradesh, India

Farooq Ahmad Dar[1] · Javid Ahmad Ganai[1] · Shakeel Ahmed[2] · M. Satyanarayanan[2]

Abstract Groundwater trace element geochemistry was evaluated in the Narji Limestone which possesses a range of substituted trace elements in the mineral matrix. The data indicate three interrelated processes control water–rock interactions and elemental concentrations in this aquifer. Dissolution influenced by pH–Eh, recharge processes and residence time controls Ca^{2+}, Mg^{2+}, Mn, Al, Cd, Ba, Sr, Co, Li, Rb, V, Fe, Pb, As, Si and Cu concentrations, while the weathering of quartzites and shales releases minute quantities of Na^+, K^+, Cl^-, Si and F into groundwater. A significant amount of Na^+, K^+, Cl^-, NO_3^-, SO_4^{2-}, Al, Fe, Cd, As, Pb, Ni, Zn, Mn, Sr, Cl, Br, Sb, Ag, Mo, Co and Cu has leached into groundwater from the use of fertilizers/manures and decayed organic matter in cultivated areas. High evapotranspiration has concentrated the chemicals by about 84%. Urbanization, land-use changes, mining and local industries have significantly increased Cd, Se, Ni, Zn, V, Fe, Cd, Sb, Ag and Cr concentrations in groundwater. The composition of groundwater is also affected by sewage, waste disposal and industrial and commercial activities. The chemical properties of about 18% of groundwater samples suggest the role of dissolution/weathering, 46% of samples have been influenced by the effects of evaporation and agricultural activities while 29% of the samples have been affected by natural hydrogeochemical processes and the effects of agricultural and industrial contamination. The quality of groundwater in the area generally conforms to the WHO recommended limits for drinking. Increasing anthropogenic interactions are likely to degrade the groundwater as karst is highly prone to contamination. This demands further investigations to ensure that the groundwater remains suitable for its intended uses in the future.

Keywords Trace element · Geochemistry · Quality · Limestone · India

Introduction

Groundwater chemistry is generally evaluated in terms of its total dissolved solid content, a measure of the amount of dissolved inorganic chemical constituents in the water. Major and secondary ingredients occur in higher and highly variable proportions while trace constituents such as metals normally occur in minute quantities generally in micrograms per liter concentrations in water. The study of trace elements has become increasingly important because of their importance for living organisms as they play vital role in certain metabolic activities. However, elevated concentrations of some trace elements are potentially dangerous environmental toxins and have claimed many lives due to fatal disease such as Minamata (mercury poisoning), Itai–Itai (cadmium poisoning), fluorosis, lead and arsenic poisoning.

Drinking water is one of the main suppliers of the major and the trace elements to plants and the animals. For the dietary requirement of humans, it contributes an estimated 40% of fluoride, 20% chromium, 19% lead, 14% calcium, 13% copper and 10% of each of arsenic and selenium (WHO 1996). Governed by an assortment of water–rock

✉ Farooq Ahmad Dar
farooq.dar1@gmail.com;
farooqdar@kashmiruniversity.ac.in

1 Department of Earth Sciences, University of Kashmir, Srinagar 190006, India

2 CSIR-National Geophysical Research Institute, Hyderabad 500606, India

🌀 Springer

interaction and geochemical processes, mineral matter of aquifers naturally releases low concentrations of many trace elements to groundwater, a key drinking water source for a large proportion of the world's population. However, higher as well as potentially dangerous concentrations of trace elements in groundwater may also be due to a wide range of anthropogenic factors such as industrial effluents (Levins and Gosk 2008; Deng et al. 2011; Purushotham et al. 2013), fertilizer/pesticide applications (Adriano 2001; Long et al. 2012), domestic waste (Li et al. 2010), petroleum products (Fels 1999) and road tar (Farmaki and Thomaidis 2008). Furthermore, metallic elements which are stable and most persistent contaminants in the environment (Chai et al. 2010; Li et al. 2014) can be progressively accumulated in animal/human bodies with time (Chengxiang et al. 2012). The concentrations of these elements in excess of their threshold values in the biological system may be harmful to flora and fauna as well as a potential cause of many fatal health concerns for humans. A wide range of the literature highlights the sources and the role of trace elements in the environment (e.g., WHO 2006; Underwood 2012; USEPA 2011).

Keeping in view their importance to animal and plant life, it is imperative to assess the sources and mobility of trace elements, identify the processes and appraise the level of contamination in groundwater to safeguard public health. For this reason, the hydrochemistry of groundwater from the Narji Limestone aquifer, which underlies an area 4333 km^2 of Andhra Pradesh, India, was assessed because the aquifer supplies water for drinking, irrigation and domestic uses of a large population. The hydrogeology of the area is also poorly understood and groundwater use is poorly managed (Dar et al. 2011, 2014a, b; 2015). In addition, chemical data act as a tracer (Barbieri and Morotti 2003; Brown and Glynn 2003; Wang et al. 2006; Bicalho et al. 2012; Gonneea et al. 2014) and is used to evaluate the hydrogeological properties of this karst system.

Study area

The study area, a flat plain with scattered mesa and butte hills, lies in the Kurnool District of Andhra Pradesh (Fig. 1). The surface elevation of the area varies from 225 to 410 m above sea level. The ephemeral Pal-Eru stream of the Kundu River drains it. Summer days are hot and dry (temperature reaches ~45 °C). More than 60% of mean annual rainfall (~700 mm) occurs in the SW monsoon (June–September) period. The annual potential evapotranspiration of the area is 1840 mm. The area is underlain by black and brownish calcareous and alkaline soils which are generally <2 m thick and up to 9 m thick in the northeastern parts of the area (Dar et al. 2011, 2015). Natural

vegetation (mainly *Prosopis juliflora*) is sparse while crops grown are rain-fed and irrigated. Irrigation from the Owk reservoir favors round-the-year paddy cultivation in the northern part of the area.

The bluish gray Narji Limestone is up to 200 m in thickness and is underlain by the Banganapalle Quartzite and overlain by Owk Shale and Paniam Quartzite (Dar et al. 2011). Older rocks of the Cuddapah Supergroup also outcrop in some parts of the study area. The upper part of the limestone is highly siliceous with thin lenses of ferruginous sandstone, and the lower sections show interbedded shale, quartzite and intraformational conglomerates (Dutt 1962). Bedding planes dip 0°–10° toward the NE. Aquifer geometry is highly complex and fast allogenic recharge occurs through karst features largely exposed in southern area, and diffuse infiltration through thick soils in the north and NE areas (Dar et al. 2014b). Drinking and domestic water is mostly supplied through groundwater with a small proportion of reservoir water.

The uppermost flaggy section of the limestone has very regular 5–10-cm-thick beds which are mined for flooring and roofing material. Cement industries and slab quarrying generate huge amounts of crushed rock waste and are progressively converting the area into bare/fallow land (Rao et al. 2001; Mouli et al. 2012). Groundwater is exploited at an increasing rate and is degrading in quality. The area of land where groundwater is used for irrigation is increasing at an average rate of 1×10^5 ha/year and surface water utilization is diminishing (Statistical Abstracts 1966–1997). The population of the area is increasing at a rate of 18%, leading to urbanization and the generation of huge volumes of domestic wastes. The region is also important for industrial and chemical manufacturing (MSME-Development Institute 2011) which produce large amounts of solid and liquid wastes likely to leach a range of chemicals into the groundwater.

Data and methodology

Seventeen (17) groundwater samples were collected in February 2011 from 13 bore wells and four karst springs of the Narji Limestone (Fig. 1) and were analyzed. Samples were collected from springs including Belum (S1) and Rati (S6) and permanent springs at Kona (S2) and Yaganti (S8). Filtered water samples were collected in properly rinsed 60-ml bottles and were acidified to a pH < 2 by adding two drops of HNO_3 to preserve the trace elements as per standards (USEPA 1989). Analysis was done by the HRICP-MS instrument at Geochemistry Division, CSIR-National Geophysical Research Institute for 21 trace elements (Li, Al, Si, V, Cr, Mn, Fe, Ni, Co, Cu, Zn, As, Se, Rb, Sr, Mo, Ag, Cd, Sb, Ba and Pb). The detection limit
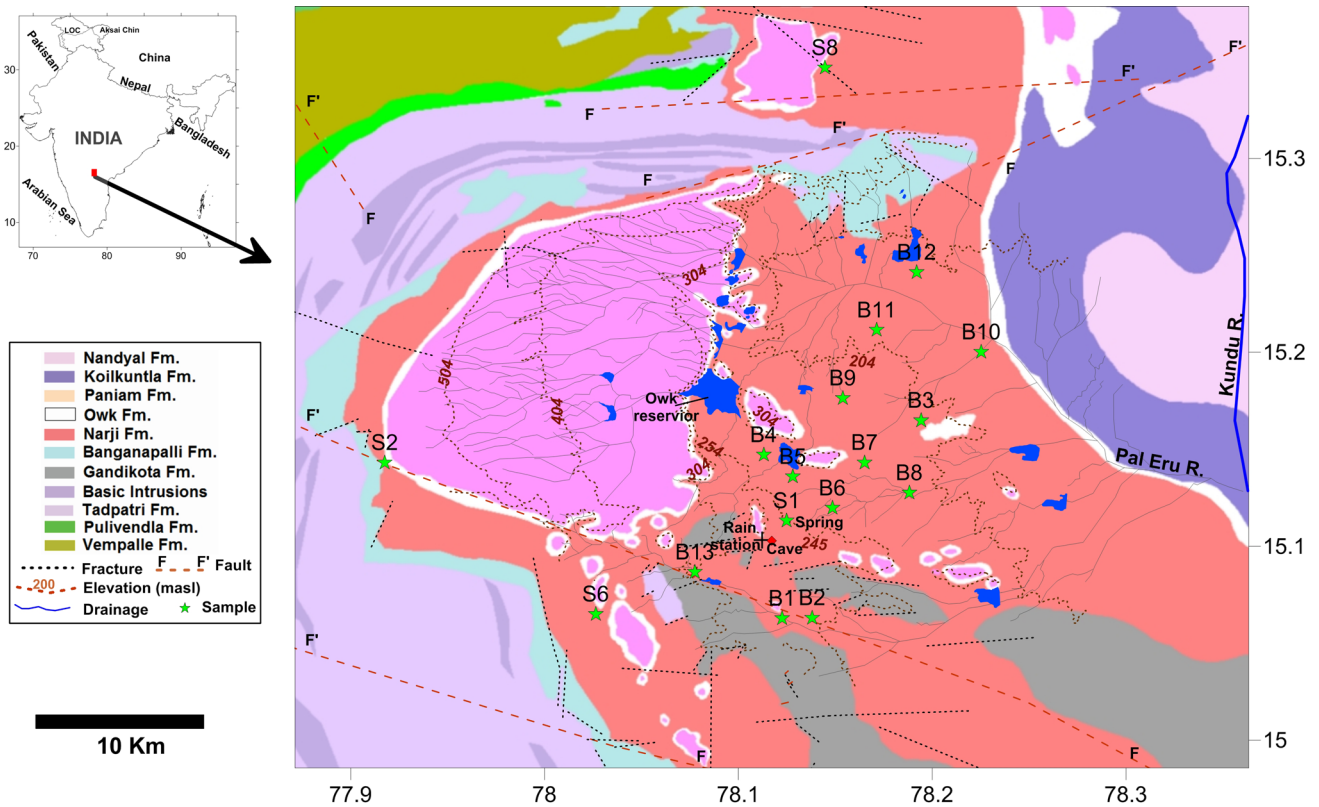
Fig. 1 Location map of the study area in India, showing geology, drainage, water bodies, fractures, faults and topographic elevation. Samples are in green symbols

was about 0.01 μg with a precision of 5%. A total of 36 parameters are discussed in this paper that include physicochemical parameters (T, pH, EC, TDS), major ions (Ca^{2+}, Mg^{2+}, Na^+, K^+, HCO_3^-, F^-, Cl^-, Br^-, NO_3^- SO_4^{2-} and phosphate) and trace elements. Limestone rock chemistry data were obtained from the published literature. The data were checked for normal distribution by assessing skewness and using the Shapiro–Wilk method (Shapiro and Wilk 1965). Out of 634 values in the entire dataset, 18 were found to be outliers that were removed before doing statistical analysis. Multivariate correlation analysis was used to find the association between different variables. Correlation coefficient (Pearson r) and *p*-values were used to evaluate the linear correlations between parameters, and probability *p*-values equal or less than 0.05 were considered to be statistically significant.

Results

The chemical composition of the host rock is an important source of chemical constituents in groundwater. Limestone composition is highly variable and depends on the salinity, turbidity, nutrient supply, fossil content, temperature and light intensity of the marine depositional environments. Carbonate rocks are generally composed of three major minerals (calcite, dolomite and aragonite) and their associated members (Table 1). Their composition depends on mineralogy, partition coefficients and enrichment factor of individual elements and ion exchange processes during deposition. Data on the major ion chemical composition of the Narji Limestone rock samples were obtained from previous studies (Kamal 1974; Vijayam et al. 1981; Kumar 1983; Bhaskar 2009; Rao et al. 2011; and references therein) as were limited information on the trace element composition of these rocks (e.g., Raju et al. 1993; Zachariah et al. 1999; Sunitha et al. 2014). The Narji Limestone compositional data are summarized in Table 2.

The variability of groundwater physical parameters and major ion data of the samples (Dar et al. 2014b) is also discussed along with trace element data. The statistical results of various trace elemental concentrations in the groundwater are given in Table 3. Li was detected at only 7 sites. Like major ions, most of the trace elements are lower in concentration than documented by other studies in the aquifer (e.g., Rao et al. 2001; Rafi et al. 2012, Table 4).

Table 1 Major mineral groups and their associated members generally found in carbonate rocks

Group	Major composition	Common impurities	Members
Calcite	$CaCO_3$	Mn, Fe, Zn, Co, Sr, Pb, Mg, Cu, Al, Ni, V, Cr, Mo	Gaspeite [Ni,Mg,Fe)CO_3], magnesite [$MgCO_3$], otavite [$CdCO_3$], rhodochrosite [$MnCO_3$], siderite [$FeCO_3$], smithsonite [$ZnCO_3$], spherocobaltite [$CoCO_3$]
Dolomite	$CaMg(CO_3)_2$	Fe, Mn, Co, Pb, Zn	Ankerite [Ca(Fe,Mg)$(CO_3)_2$], kutnohorite [Ca(Mn,Mg,Fe)$(CO_3)_2$], minrecordite [$CaZn(CO_3)_2$], norsethite [$BaMg(CO_3)_2$]
Aragonite	$CaCO_3$	Sr, Ba, Pb and Zn	Cerussite ($PbCO_3$), strontianite ($SrCO_3$), witherite ($BaCO_3$)

Table 2 Chemical composition (range/mean in weight%) of Narji Limestone rock samples compiled from the literature

Oxide	Rao et al. (2011)	Kamal (1974)	Jeyagopal et al. (2006)	GSI 1986 (cited in Sengupta 2007)
LOI	29.94–40.64/34.73	5.43–39.72/27.60	29.88–37.74/34.67	29.86
SiO_2	6.14–27.18/17.68	8.58–70.68/29.81	10.8–28.8/18.22	15.88
Al_2O_3	0.49–2.27/1.18	0.6–19.2/4.98	1.05–2.49/1.06	6.79
Fe_2O_3	0.25–2.4/0.86	0.38–8.01/2.97	0.04–33/0.11	8.69
CaO	37.93–50.78/43.65	3.29–59.08/35.14	37.03–46.01/43.23	34.06
MgO	0.15–1.3/0.59	0.2–0.72/0.43	0.39–1.46/0.91	1.08
Na_2O	0.07–0.31/0.19	NA	0.55–0.78	NA
K_2O	0.16–0.5/0.3	NA	0.15–0.39	1.43
FeO	NA	NA	0.29–0.68	NA
P_2O_5	NA	NA	0.16–0.18	0.03
TiO_2	0.02–0.16/0.06	NA	0.03–0.08	0.26
MnO	0.01–0.04/0.02	NA	0.02–0.05/0.03	1.71
S	NA	NA	NA	0.005
Cr_2O_3	NA	NA	NA	0.01
BaO	NA	NA	NA	0.19

Discussion

Geochemistry of Narji Limestone

From the previous geochemical studies and published data as summarized in Table 2, it is observed that the Narji Limestone is composed primarily of calcite with lesser amounts of dolomite and aragonite (Dar et al. 2011). The binary relation between CaO and MgO data (Kamal 1974) indicates that the carbonate formation purely lies in the limestone field with MgO value lying below 2%. The average content of CaO is ∼34.6%, MgO is ∼0.5% and total carbonate as $CaCO_3 + MgCO_3$ is ∼60.5% (Kumar 1983; Rao et al. 2011). This is analogous with the results of limestone rock analysis from the southern parts of the Cuddapah Basin (south of the study area) which show 43–49% CaO, 9–15% silica and <2% MgO (Bhaskar 2009) as well as in the northern parts (north of the study area) with CaO 37.03–46.01%, MgO 0.39–3.35% and SiO_2 10.8–28.8% (Jeyagopal et al. 2006). Published geochemical data

were converted to weight% of the major oxides: carbonate, silicate and clay content, reduced to a set of chemical components [CaO], [MgO], [SiO_2] and [Al_2O_3] in mole units and normalized to mole fractions in 100%. For example, the mole fraction of N(CaO) is expressed as:

$$N(CaO) = \frac{[CaO]}{[CaO] + [MgO] + [SiO_2] + [Al_2O_3]}$$

The sum of N(CaO) + N(MgO) represents the total carbonate content in the rock. The clay and silicate content of limestones is generally represented by kaolinite ($Al_4Si_4O_{10}(OH)_8$) from which Al_2O_3 and SiO_2 were deduced as Al and Si which occur in 1:1 ratio in kaolinite (or 1:2 ratio as two oxides). Normalized carbonate, silica and clay were plotted in a trilinear diagram (Fig. 2) which also shows that the limestone is dominantly composed of calcite, with up to 10% of dolomite and less than 40% silica and clay (Vijayam et al. 1981). The calcite is fine-grained with diagenetic fine calcite in micro-veins. Anhedral calcite crystals and silicate inclusions occur in patches. The limestone is

Table 3 Statistics of trace elemental concentration of 17 groundwater samples of the Narji Limestone aquifer

Trace element	Min	Max	Mean ± SD	Skewness	Median	WHO standard	Pollution index (%)
Al	4.94	228.79	52.43 ± 70.78	1.76	16.81	200	26.2
Si	2.09	9.99	4.56 ± 1.73	1.94	4.09	NG	–
V	0.52	3.47	1.10 ± 0.80	2.21	0.85	5000	0.03
Cr	11.58	13.16	12.54 ± 0.42	−0.70	12.51	50	25.1
Mn	0.25	27.30	4.37 ± 6.69	3.05	3.02	400	1.1
Fe	28.07	196.64	80.52 ± 54.25	1.14	59.29	300	26.8
Ni	0.45	3.14	1.23 ± 0.75	1.39	0.93	70	1.7
Co	0.03	0.24	0.08 ± 0.06	1.81	0.06	70	0.1
Cu	0.85	2.29	1.49 ± 0.48	0.44	1.44	2000	0.1
Zn	5.22	94.34	41.52 ± 30.60	0.27	31.34	3000	1.4
As	0.10	0.40	0.19 ± 0.09	1.36	0.17	10	1.9
Se	0.26	3.70	1.06 ± 0.95	2.05	0.72	40	2.6
Rb	0.07	0.71	0.26 ± 0.20	1.06	0.18	NG	–
Sr	34.70	294.57	100.77 ± 72.79	1.72	82.31	NG	–
Mo	0.09	0.59	0.32 ± 0.15	0.34	0.27	70	0.4
Ag	0.002	0.010	0.006 ± 0.003	0.77	0.005	100	0.01
Cd	0.01	0.07	0.03 ± 0.02	0.74	0.03	3	1
Sb	0.01	0.06	0.03 ± 0.01	1.12	0.02	20	0.1
Ba	2.88	57.50	20.21 ± 16.80	1.25	13.85	700	2.9
Pb	0.31	2.45	1.14 ± 0.54	0.92	1.06	10	11.4

Units are in micrograms/l (μg/l). WHO recommended values and calculated pollution index of each parameter are also given

NG No guidelines, because they occur in drinking water at concentrations below those of health concern

unfossiliferous. The Mg content of the limestone is likely to have been derived from magnesium-containing debris or from post-depositional alterations (Rao et al. 2011). The free silica includes quartz grains or chert and medium-grained quartz is detrital in origin.

The limestone is rich in clay and contains a considerable quantity of pyrite both as fine crystals disseminated throughout the rock matrix and as large euhedral FeS_2 crystals (Sarkar et al. 2010). The high sulfide content of the limestone is an indicator of its impurity and the anoxic as well as iron-enriched depositional environment in which it was formed. A few samples in the right corner of Fig. 2 with high silica and clay contents might represent the upper flaggy and lower variegated depth units of the limestone. The formation varies in properties/composition from top-most flaggy part (~5 m thick) to middle massive limestone (up to 30 m thick) and to lower variegated unit (~65 m thick) which have 40–42%, 44–49% and 38–42% [CaO], respectively (Bhaskar 2009).

The limestone samples possess high to very high contents of Fe, small amounts of Na, Mg, Al, Mn and B and traces of Ti and V (Vijayam et al. 1981). Higher SiO_2 and Al_2O_3 levels by comparison with average global limestones indicate the siliceous- and argillaceous-rich character of this formation (Jeyagopal et al. 2006) as evident

from higher K (or clay) particularly in upper units (Bertram 2010). Mn and V generally accumulate during deposition and digenesis (Breit and Wanty 1991) and are typically from terrestrially derived sources (Gonneea et al. 2014). Sr is the primary element in limestones that occurs either as celestine [$SrSO_4$] or as strontianite [$SrCO_3$] (Wong et al. 2012). Likewise, witherite [$BaCO_3$] is common mineral in carbonate environments and contains various substituted metals. The limestone is also rich in barite [$BaSO_4$] as common mineral because of its stable nature over vide range of pressure and temperature of the crust (Sarkar et al. 2010) and may also contain Sr, Ca, K, Ra, Pb and rare earth element (REE) with minor substitution of Fe, Cu, Zn, Ag, Ni, Hg and V in variable proportions (Griffith and Paytan 2012). Zoisite, tremolite, pitchblende and coffinite are also reported to occur in the Narji Limestone containing a range of trace elements (Raju et al. 1993; Zachariah et al. 1999). Elements such as Nd, Pb and U are admixed with the siliceous and phosphate content of the Narji Limestone. U (0.4–1.6 ppm) and Th (0.3–27.1 ppm) are also reported to occur in this formation (Bertram 2010), and the elevated levels of Pb may occur as the by-product of radioactive decay of both elements.

Furthermore, the overlying shales and quartzites possess a range of non-carbonate minerals such as barite [$BaSO_4$],

Table 4 Data showing concentrations of major and some trace metals in different water types of this limestone region

Element	Groundwater (mg/l)	Surface water (mg/l)	Tap water (mg/l)
TDS	74–14180 (a); 1053–4448 (b)		
Na^+	2.5–1813 (a); 139–480 (b)		
K^+	0.09–1058 (a); 2–10 (b)		
Ca^{2+}	7–553 (a); 134–688 (b)		
Mg^{2+}	1–267 (a); 60–233 (b)		
Cl^-	10–4500 (a); 345–1400 (b)		
SO_4^{2-}	5–2500 (a); 77 (b)		
HCO_3^-	5–1168 (a); 308–1000 (b)		
CO_3^{2-}	0.5–87 (a); 180 (b)		
NO_3^-	600–1000 (c); 26 (b)		
F^-	0.05–4 (a); 1–1.5 (b); 0–11.5 (c)		

Element	Groundwater (µg/l)	Surface water (µg/l)	Tap water (µg/l)
Cu	2–170 (a); 1470–2670 (d)	1250–1980 (d)	1980–2960 (d)
Zn	1–10200 (a); 11000–19000 (d)	5000–8000 (d)	9000–13000 (d)
Al	80–150 (d)	70–100 (d)	120–180 (d)
Mn	1–1666 (a); 60–630 (d)	40–230 (d)	70–410 (d)
Fe	10–75720 (a); 600–940 (d)	80–250 (d)	270–480 (d)
U	0.5–100 (a)		
Si	4–117 (a)		
Ba	5–900 (a)		

(a) Singh et al. (2002); (b) CGWB (2011) (c) Babu Rao et al. (2001); (d) Rafi et al. (2012)

steatite $[Mg_3(Si_4O_{10})(OH)_2]$, chrysotile asbestos $[Mg_3(Si_2O_5)(OH)_4]$ and uranite $[UO_2]$ (Sunitha et al. 2014). The laterally extensive Owk Shale (10–12 m thick) also has a thin rhyolitic tuffacious layer rich in quartz, biotite, muscovite, chlorite, siderite and iron oxides such as limonite (Saha and Tripathy 2012). This unit contains elevated concentrations of TiO_2, Al_2O_3, FeO, Fe_2O_3, Th, Ba and U and low levels of alkali and alkaline earth elements (Na_2O, K_2O and CaO) that has extensively leached and caused fluidization of Narji Limestone as observed by brecciation and vent features in the bedding planes (Patranabis-Deb et al. 2012). This process has increased the amount of many trace elements in the original limestone.

Hence, the limestone possesses variable quantities of trace elements incorporated during deposition and digenetic alteration commonly by substitution of Ca^{2+}, Mg^{2+}, etc. due to similarity in charge, ionic radius and electronegativity alike other carbonate units of the Cuddapah Basin such as Vempalli dolomite which possess higher than normal values of Mo, V, Cu, Co, Ni, Pb, U (Rai et al. 2011) as well as carbonates of the world (Gascoyne 1983; Morse and Mackenzie 1990; Hem 1985).

Since weathering/dissolution of the limestone and other rock types by groundwater is thermodynamically a continuous process, the varying amounts of a range of trace

elements is likely to enter the groundwater system of this region (Radell and Katz 1991).

Groundwater physical parameters and major elements

Physicochemical variables and the chemical composition of groundwater of the study area, as statistically summarized in Table 5, are also discussed in Dar et al. (2014b). Groundwater levels in the limestone aquifer are highly variable, with a lowest value 182.8 m asl at B10 and a highest 277.3 m asl at B1. Spring S1 has water level of 263 m asl (8 m bgl). This water level has a higher mean value (225 ± 31 m asl) than median (216 m asl), a low coefficient of variation (14%) and a skewness ≈ 1. Groundwater flow direction is generally toward northeast. No significant correlation arises between water levels and other variables except for a relationship with temperature (R^2 0.8) and Ba (R^2 0.5). But at lower R^2 values Na, sulfate and Mo concentrations decrease with increase in water levels (respective R^2 values are −0.4, −0.5 and −0.4).

Water temperature remains high in the area and ranges from 27.9 °C at B9 to a high of 32.5 °C at B2. High water temperatures (average 30 ± 1.5 °C) are due to high ambient atmospheric temperature which even reaches
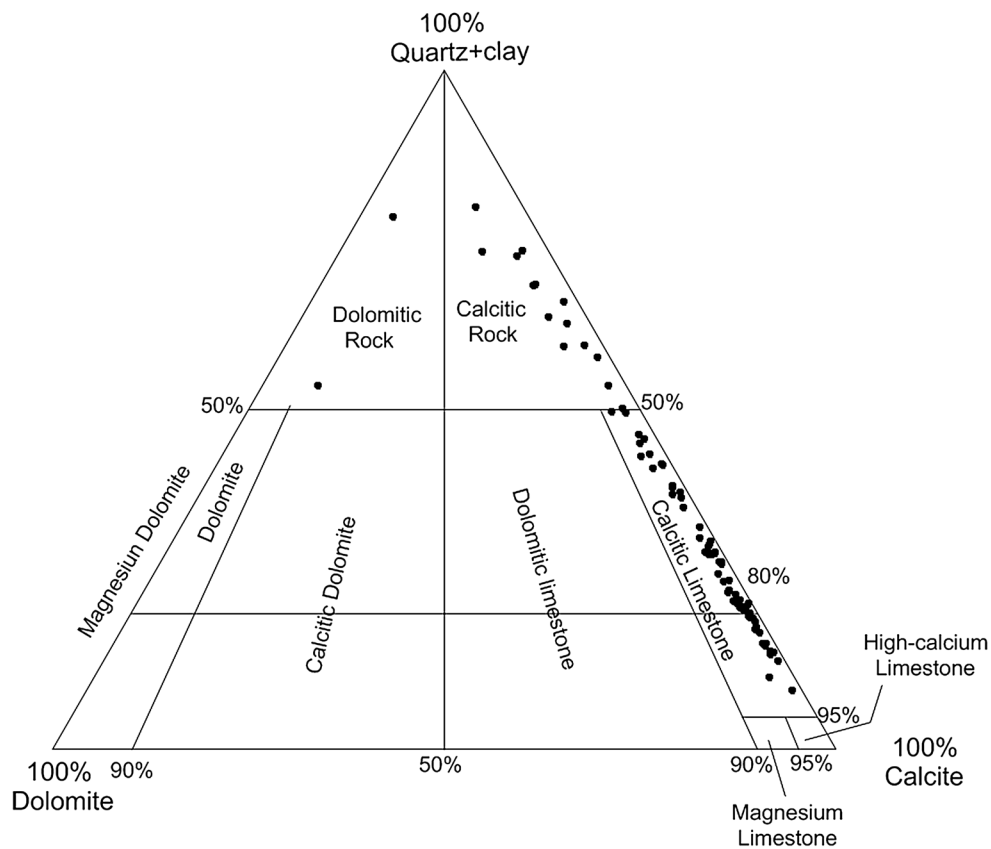
Fig. 2 Triangular plot of the Narji Limestone rock composition expressed as three components (carbonates, clays and silica). Limestone is calcitic in character with significant amounts of silica and minute dolomitic content

45 °C in summer months. Temperature shows less spatial variability (CV 4.9%) and normal distribution (skewness < 1). Strong correlations (Table 6) of temperature with Pb and moderate correlations with Mg, Na and Se indicates its control on dissolution as these elements are commonly found in limestones as documented in karst systems elsewhere (Gascoyne 1983; Singh et al. 2002). Groundwater is mildly acidic to slightly alkaline with pH of 6.74 in B5 and alkaline pH of 7.67 in S6 water. pH shows less variability with small differences between mean (7.0 ± 0.24) and median values (Table 5). NO_3^- concentrations are highest in the samples with low pH, i.e., acidic water ($R^2 = -0.4$) indicating the role of anthropogenic processes. The lowest EC value of 538μS/cm (TDS ≈ 370.95 mg/l) corresponding to freshwater was measured in S6, and the highest EC value of 3890 μS/cm (TDS ≈ 3010.47 mg/l) was measured in B7. Values of EC have a large range in the aquifer with 68.3% CV (Fig. 3), mean value (1329 ± 907μS/cm) > median and skewness 1.8. EC is significantly correlated with a majority of the analyzed elements (Table 6) reflecting its natural origin in the aquifer. A moderate correlation of EC with Si, Fe, Zn, As, Sr and Pb ($R^2 > 0.5$) is related to the weathering of mineral matter,

and anthropogenic sources such as Cu, F, Fe, Zn, Pb and Se also occur in domestic waste.

Major ions with CV < 50% (Fig. 3) include F^- > Mg^{2+} > Ca^{2+} > HCO_3^-. Although the range of Ca^{2+} (31.19 mg/l at B10 to 123.38 mg/l in B9), Mg^+ (16.82 mg/l at B8 to 53.81 mg/l at B12) and HCO_3^- (205 mg/l at B7 and 710.63 mg/l at B12) is large, they show a low degree of variability from site to site with small difference of mean and median and a similar level of skewness (Table 5). This reflects that the sources of these ions are identical from site to site with only a minor degree of variation expected from human factors. Average concentrations of Ca^{2+} and HCO_3^- are 74 ± 25 mg/l and 477 ± 162 mg/l, respectively. Concentration of Ca^{2+} up to 668 mg/l has been found by other studies (Table 4).

The dissolution of carbonate minerals is the main source of Ca, Mg and HCO_3^- as the groundwater is generally saturated with respect to $CaCO_3$ (Dar et al. 2014b) and CaO is the dominant oxide in the limestone (Table 2). The dolomitic content (MgO < 2%) causes high Mg in groundwater (29 ± 11 mg/l) as observed by other studies also in the range of 1–233 mg/l (Table 4). Mg^{2+} might also be released from magnesium fused phosphate fertilizers (Bolland et al. 2005). A strong correlation of Mg and

Table 5 Statistical data of in situ parameters and major ions of 17 groundwater samples of the Narji Limestone

Parameter/Major ion	Min	Max	Mean ± SD	Skewness	Median	WHO standard	Pollution index (%)
WL mbgl	1.32	21.80	8.47 ± 6.2	1.02	7.73	–	–
T (°C)	27.90	32.50	30 ± 1.5	0.86	29.35	NG	–
pH	6.74	7.67	7 ± 0.24	0.20	7.14	NG	–
EC (μS/cm)	538.00	3890	1329 ± 907.4	1.83	916.50	NG	–
TDS	370.95	3010.47	976 ± 729.1	1.81	631.93	2000	48.8
Ca^{2+}	31.19	123.38	74 ± 25.47	0.54	71.30	NG	–
Mg^{2+}	16.82	53.81	29 ± 11.1	0.65	27.61	NG	–
Na^+	34.13	406.10	163 ± 123.7	1.08	120.17	200	81.5
K^+	1.56	31.77	10 ± 8.55	1.43	7.49	NG	–
F^-	0.39	2.29	1 ± 0.49	1.26	0.90	1.5	70.5
Cl^-	13.07	368.22	132 ± 109.7	1.06	75.76	1000	13.2
Br^-	0.23	4.18	1.4 ± 1.19	1.40	0.84	NG	–
Li	0.01	0.09	0.04 ± 0.03	0.61	0.04	NG	–
HCO_3^-	205.00	710.63	477 ± 162.8	-0.18	537.10	NG	–
NO_3^-	4.39	255.82	61 ± 77.04	1.79	26.44	100	60.6
SO_4^-	2.85	167.96	56 ± 53.4	0.76	23.58	500	11.1
TH	163.78	386.30	305 ± 57.3	-0.84	316.27	600	50.8
PO_4^-	1.03	2.39	1.6 ± 0.7	1.28	1.37	NG	–

WHO recommended values and calculated pollution index of each parameter are also given

NG No guidelines, because they occur in drinking water at concentrations below those of health concern

HCO_3^- and a negative association between Ca and Mg suggest a decoupling process is taking place driven by differences in the rate of dissolution (Dar et al. 2014b). A negative correlation of Ca with Mg, HCO_3^-, Cd and Pb and positive association with SO_4^{2-} as well as positive correlation of Mg with all these variables could also be explained by decoupling in the carbonate system.

The lowest fluoride concentration of 0.39 mg/l was measured at S6, and maximum concentration of 2.29 mg/l was measured at site B9. The average concentration is high (mean 1.0 ± 0.5 mg/l). Fluoride concentrations as high as 11.5 mg/l have been reported in this karst area (Table 4). The most common source of fluoride in groundwater is the weathering of rocks containing F-bearing minerals, particularly calcium fluoride. F is typically associated with Si and Sr which are commonly found in limestones, quartzites and shales. The positive association with Mg^{2+} and HCO_3^- suggests that the source of this ion is the dissolution of fluorite. Groundwater U of <1 to 100 ppb (Singh et al. 2002) and F–U relation also suggests this process is taking place (Langmuir 1978). A low variability (CV 46.7%) suggests the strong solubility control of fluorite in a buffered pH system. Fluoride concentrations in groundwater are also increased by high evapotranspiration (Dar et al. 2014b).

Nitrate, sulfate, bromide, potassium, chloride and sodium ions have large concentrations with a high degree

of variability in groundwater in the area as shown in Fig. 3 and Table 5. This variability suggests that they are derived from multiple sources such as weathering of carbonates and other rock types, fertilizer application, sewage and organic matter. Nitrate concentrations range from a minimum of 7 mg/l at S2 to as high as 256 mg/l in B9 with average 61 ± 77 mg/l. Similarly, sulfate concentrations range from a low of 3 mg/l in S2 to a high of 168 mg/l in B10 with mean 56 ± 53 mg/l. Sulfate in groundwater from karstic aquifers is typically derived from the oxidation and weathering of pyrite in the limestone. Ca has a strong positive correlation with SO_4^{2-} and a strong negative correlation with Mg, HCO_3^- and F ($R^2 > -0.6$) which also suggests that sulfate is mainly from limestone. Elevated concentrations of NO_3^- and SO_4^{2-} in groundwater may be derived from fertilizers (urea, calcium superphosphate and potassium sulfate), liquid sprays and manures as well as from degraded organic matter and domestic wastes. In this karst area, fertilizers containing 20 kg N, 40 kg P_2O_5 and 40 kg K_2O and agrochemical sprays for pest and fungi control are widely applied for crop management (Vittal et al. 2005).

The lowest measured concentration of Na^+ (34 mg/l) was at site S2 and the highest concentration of 406 mg/l at B12 with an average concentration of 163 ± 124 mg/l. K^+ varies from 2 mg/l at B4 to 23 at B6 with average 8 ± 7 mg/l. Na and K are highly mobile elements and are

Table 6 Pearson correlation matrix of various geochemical parameters of groundwater

	T	EC	Ca	Mg	HCO₃⁻	Na	K	F	Cl	NO3	SO4	Br	Si	V	Cr	Mn	Fe	Ni	Co	Cu	Zn	As	Se	Sr	Mo	Ag
Mg	0.56	0.56	0.63																							
HCO₃⁻	0.67		0.73	0.91																						
Na				0.73	0.55																					
K																										
F		0.71	0.67	0.68	0.63	0.63																				
Cl																										
NO3																										
SO4			0.70						0.67																	
Br									0.79																	
Al		0.52								0.61		0.58														
Si		0.51	0.53	0.79	0.72	0.52		0.82																		
V				0.58									0.81													
Cr			0.54	0.58	0.71					0.75	0.68															
Mn	0.51				0.57	0.74																				
Fe		0.54					0.64									0.63										
Ni																0.81	0.80									
Co																	0.73	0.90								
Cu		0.79					0.53		0.56	0.57							0.89	0.60	0.55							
Zn		0.54		0.63	0.62	0.69	0.61	0.61					0.90	0.88						0.69						
As		0.53		0.64	0.60	0.52		0.65					0.57							0.65	0.52					
Se	0.55	0.93		0.75	0.64	0.66														0.64	0.65	0.52				
Rb																	0.68	0.90	0.75							
Sr		0.56		0.65	0.62	0.55		0.69		0.52			0.89	0.83		0.50				0.64	0.54	0.92	0.51			
Mo						0.56								0.51										0.64		
Ag									0.59								0.64			0.76						
Cd			0.66																							
Sb						0.69			0.81	0.68										0.58			0.51			0.74
Ba	0.62			0.83	0.74	0.87					0.63		0.66			0.89			0.74				0.78	0.54	0.64	
Pb	0.82	0.59	0.50		0.74	0.62		0.61					0.66		0.59											

R^2 value > 0.5 corresponding to moderate to very high correlation is considered

Bold green-highlighted values represent significant correlation ($R^2 > 0.65$); red values represent significant negative correlations
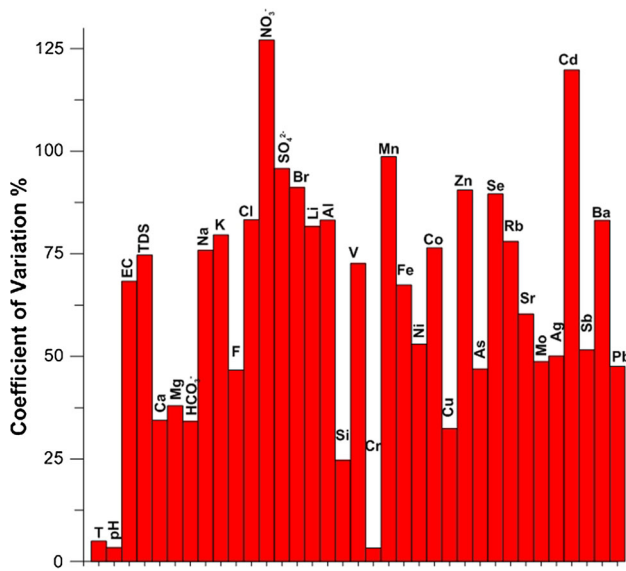
Fig. 3 Bar plot showing the percentage coefficient of variability (CV) of various parameters analyzed in groundwater

released into groundwater from weathering of minerals in limestone which contains average Na_2O and K_2O levels of 0.48 and 0.3 wt%, respectively (Table 2). In addition, the elements are also likely to enter groundwater from the weathering of overlying shales and quartzites through runoff and subsequent infiltration. Other sources of these ions in groundwater include leaching from fertilizers, manures and other human sources.

Similarly, the lowest concentration of Cl^- in groundwater was 13 mg/l measured at site S2 and the highest level of 368 mg/l at site B12 with an average concentration of 132 ± 110 mg/l. High concentrations of Cl^- in groundwater are clearly associated with evaporative losses and anthropogenic contamination with likely inputs from the weathering of rock minerals. Average $[Cl^-]$ from atmospheric sources is generally below 1 mg/l (rainfall Cl^- ranges from 0.2 to 0.8 mg/l). Concentrations of Br^- vary from 0.2 mg/l (B4) to 4.18 mg/l (S8) with an average concentration 1.4 ± 1 mg/l. Br is geochemically similar to Cl and is mainly derived geogenically from minerals and observed by its correlation with Cl and Al ($R^2 = 0.79$). However, its high variability may also indicate that there are some anthropogenic sources of this element.

Groundwater in the study area also possesses high values of total hardness (mean 305 ± 57 mg/l of $CaCO_3$) that ranges from 164 mg/l (B10) to 386 mg/l (S6). Phosphate was detected only in three sites (1.03 mg/l at B12, 1.37 mg/l at B10 and 2.39 mg/l at B11). High phosphate above 1 mg/L (average 2 ± 0.7 mg/l) of karst groundwater suggests the release from P_2O_5 content of the limestone (Table 2) and contamination from fertilizers and human/animal wastes (Kilroy and Coxon 2004; Long et al. 2012).

Most of the parameters are found in comparably lower ranges than documented by other studies (Singh et al. 2002; CGWB 2011; Rafi et al. 2012; Table 4).

Groundwater trace elements

The minimum, maximum and median values of trace element concentrations in groundwater in the study area are shown in Table 3. The elements with CV > 50% are in decreasing order Mn > Al > Se > Ba > Li > Rb > Co > Zn > V > Sr > Fe > Ni > Cd > Sb (Fig. 3) and all have CV more than 60% except for Cd and Sb. They generally possess higher mean than median values and skewness values >1 which indicate a non-normal and inhomogeneous distribution as well as a role of multiple factors on their spatial variability. Groundwater Mn concentrations vary from the lowest value of 0.25 µg/l at B5 to a high of 27.3 µg/l at B11 site with average 3 ± 3 µg/l. Mn has the highest CV and skewness by comparison with other trace elements in groundwater. The primary source of groundwater Mn is likely to be the dissolution of manganese oxides and carbonate minerals that contain Mn. The content of Mn in the Narji Limestone lies in the range of 0.01–0.05 with an average 0.02wt% in the area (Table 2). Al concentrations possess large range (4.94 µg/l at site B8 to 229 µg/l at S1 site), much higher mean than median, CV and highly skewed data. The Narji Limestone has significant proportion of Al_2O_3 ranging from 0.49 to 19.2wt% and an average 3 wt% (Table 2). Thus, primary source of Al in groundwater is likely the clay content in the aquifer matrix. Additional Al may come from surface water with Al up to 70–100 µg/l being measured in the region (Table 4). The statistical data of Se show average concentration 1 ± 0.9 µg/l. Natural source includes weathering of rocks as Se is commonly found in the range of 0.1–6 ppm (average 0.08 ppm) in limestone minerals (Adriano 2001). This is observed by strong correlation of Se with the elements commonly found in limestone minerals (Table 6). Both Zn and Se are also commonly contained in pyrite and can be co-released when pyrite is oxidized. The highest Se concentrations in groundwater occurs at B9–B13 sites and highest correlation value of 0.93 with EC also suggests that Se is associated with surface irrigation, re-evaporation and groundwater with high EC as shown in Table 6 (Deverel and Fujii 1988). Anthropogenic sources include domestic waste which generally possesses high Se levels (e.g., shampoos contain ~2.5% of selenium sulfide; Leung and Jiao 2006). Ba concentrations in the karst groundwater range from 2 µg/l at B7 to 57.5 µg/l at S2. High concentrations and variability indicate multiple sources in the groundwater as also reported by other studies in the range of 5–900 µg/l (Table 4). Alkaline earth metals (Ba and Sr) behave

geochemically similar to Ca and Mg and are primary elements in carbonates. Major sources of Ba in groundwater include the dissolution of minerals such as barite ($BaSO_4$) and witherite ($BaCO_3$) (Gonneea et al. 2014). Sr is a common constituent of carbonate minerals and is likely to have been derived from their dissolution which contributes about 15–28% to the total chemical input of Sr to oceans globally from karst waters (Gonneea et al. 2014). Weathering of plagioclase feldspars in quartzites also releases Sr (Leung and Jiao 2006). A negative relationship of both Mn and Ba with Na, and Mn with Co and Ba as well as a negative correlation of NO_3^- with Al, Mn and Ba suggests a lithogenic source of Ba, Mn, Co, Al as they are generally associated with carbonate mineralogy. Sr may also be released from fertilizers which posses significant amounts of this element (18 ppm in potassium fertilizer; 0.11 ppm in nitrogen F; 520 ppm in phosphate F, e.g., Banner et al. 1994).

The concentration of lithium in groundwater in the study area also shows a large variability. Its average value is 0.04 mg/l and lowest was measured at S8 and highest at B11. A major source of this element is likely to include by weathering as Li behaves in a similar manner to Mg^{2+} and is present in limestone as a secondary element. The average concentration of Rb in groundwater is 0.3 ± 0.2 μg/l: 0.07 μg/l is measured at B7 site and 0.71 μg/l at S8 site. Ca and Mg are also strongly associated with the alkaline earth metal Rb (Wang et al. 2006) which is also a minor constituent of carbonate minerals. Hence, mineral dissolution is the dominant source of this element in groundwater in the area. Co is mainly from limestone as it is associated with most of the elements present in carbonate minerals as shown in Table 6 and has been found to occur up to 20 ppm in soils from limestone areas (Adriano 2001). Anthropogenic sources of Co include the use of alloys, as 75% of the global production is used in alloys (Adriano 2001). Zinc is the 24th most abundant element in the earth's crust and has a rage of <1–180 ppm (average 20 ppm) in limestones (Adriano 2001). The anthropogenic sources of zinc are common as it ranks 4th among metals in annual consumption after Fe, Al and CU. The common sources in groundwater include tire manufacturing/wearing, metal smelters and mining activities, zinc alloys, dye casting, rubber and paints (Guo et al. 2005). The main source of V in groundwater is likely to be the geogenic as the element occurs in the limestone (Vijayam et al. 1981). V correlates with As and Sr which are also present in aquifer. Anthropogenic sources of V include industrial wastes, sewage sludge and fossil fuels (Mattigod and Page 1983). Fe is the second-most abundant metal in the earth's crust and is also a common constituent in soil and groundwater systems (Deverel et al. 2012). Fe is primarily released from limestone weathering that possess Fe_2O_3

between 0.25 and 33 and average 0.86–2.97wt% (Table 2) as well as from the oxidation of pyrite present in the limestone. Paints, plastics, industrial units and water treatment facilities in which Fe is commonly used are potential anthropogenic sources of this element. The anthropogenic sources of Ni include use of alloys, stainless steel, Ni–cadmium batteries, electroplating, welding products and electronic products (IARC 1990). Cd concentrations in groundwater of the study area are 0.01 μg/l at B4 and B7 sites and 0.07 μg/l at B5, and its average is 0.03 μg/l. Cd in groundwater is primarily derived from geogenic sources as Ca- and Mg-bearing minerals are strongly associated with the element (Morse and Mackenzie 1990). Other potential sources of cadmium are of anthropogenic origin including battery processing as well as phosphate fertilizers and agrochemicals containing Cd (Deverel et al. 2012; Markovic et al. 2006). Minor sources of Cd, Ni, Zn and Sb come from villages/towns and agriculture areas as these metals are generally found in higher concentrations in domestic sewage sludge where they are present in metal–organic compounds (Adriano 2001; Berti and Jacobs 1998) and in animal manures (Deverel et al. 2012). This is suggested by positive correlations of Na with Zn and Sb (Table 6). Zn may also be derived from minerals present in the aquifer matrix as the element correlates well with Mg. The positive relationships of Cl with SO_4^{2-}, Br and Sb suggest that fertilizers and sewage are possible sources of these elements in the study area.

A number of the analyzed elements have a CV < 50% (Ag > Mo > Pb > As > Si > Cu > Cr, Fig. 3) and have small range, and mean values are near to median. Most of these elements are near normally distributed (skewness of −1 to +1). This possibly suggests that the elements are affected by a few sources in groundwater. A positive correlation of Ag with Cl, Fe, Cu and Ba suggests that this element is derived from both weathering and anthropogenic sources. The main source of Mo is likely to be anthropogenic as this element is often associated with sewage sludges and other sources of organic material (Jarrell et al. 1980). Mo may also be derived from the use of agrochemicals (Markovic et al. 2006). Pb is mainly derived from cerussite [$PbCO_3$], an associated carbonate mineral. However, it might also release from combustion of gasoline and diesel (e.g., Hooftman et al. 2016; Yao et al. 2015), leaching from well casings and use of lead arsenate pesticides (Peryea and Creger 1994). Arsenic is often derived from the geogenic sources as As is commonly found in carbonate minerals (Vanderzalm et al. 2011) as well as in clay minerals (Crites 1985) and arsenopyrite (Deverel et al. 2012). This is supported by the correlation between As, Sr and Mg (Table 6). The use of arsenical pesticides is a potential anthropogenic source of the element (Hem 1985). Si concentrations are influenced

mainly by weathering of limestone possessing high SiO_2 (6.14–70.68 wt% Table 2). Strong correlations of Ca and Mg with Si, of HCO_3^- with Si, Cr and Pb and of Si with Sr also support this view. The main source of Cu is likely to be the weathering as Cu impurities are common in calcite (Rafi et al. 2012). Anthropogenic sources of Cu include copper sulfate pesticides (Adriano 2001) and domestic sewage (Deverel et al. 2012). Cu may be leached from fertilizers and in some pesticides in the area (Cloutier et al. 2008) as observed by higher values in samples (B3, B9, B10, B11, B12) from agriculture areas. The major anthropogenic sources of groundwater Cr include sewage sludge, wastewater, metal and wood preservation units, water cooling facilities and mining activities as Cr is used as corrosion inhibitor (Adriano 2001). Cr is also a pollutant from leather industries, paints, fungicides, etc. (Hu 2002).

Thus, the concentrations of different elements are controlled or influenced in the groundwater by various processes which operate in the area as summarized in Table 7. Except for Mn, Ni, Rb, Cd and Ba, the analyzed chemical constituents are higher in wells than in springs. This suggests the role of human-, agriculture- and industry-related sources on the groundwater from well sites in the area (Radell and Katz 1991). Furthermore, samples collected from wells have higher concentrations of Al, Si, Ca, Ba, Cu, Cd, Pb and Mg, suggesting that deeper groundwater in wells (springs generally flow from higher levels of Narji Limestone) is more mineralized.

Spatial variability of groundwater data and aquifer heterogeneity

Karst aquifers intrinsically have a large degree of heterogeneity (Dar et al. 2011, 2014b) which is indicated by the variability of groundwater trace element data in the paper. Based on chemical properties determined in this study, the aquifer can be divided into three zones with significantly distinct hydrogeological characteristics. The northern part of the study area (group 1 samples) is characterized by thick soils (average thickness 1–2 m and up to 9 m at places), paddy fields, canal irrigation, large use of

fertilizers/manures, shallow water levels, diffuse recharge and decomposed organic matter. These characteristics increase the evaporation of recharging water, irrigation return flow, which gives rise to a highly mixed and chemically rich groundwater (high EC and enriched isotopes; Dar 2014). These factors are likely to have influenced water chemistry at sites B3, B7, B9, B10, B11, B12 and B13. The southern area (group 2 samples) is hydrogeologically more karstified with more rapid recharge through sinkholes and other karst features and limited diffuse recharge through intermittent and thin soils (thickness < 1 m), dominant conduit flow and mainly rainfed cultivated crops (Dar et al. 2014b). These samples include B1, B2, B4, B5, B6, B8 and S1. It has also high tourist inflow due to the famous Belum Cave near S1 (Fig. 1). A highly karstified and fractured third zone (group 3) comprises groundwater samples S2, S3, S6 and S8 with chemical signature similar to non-evaporated rainwater (Dar 2014). The area is apparently less affected by agriculture and other land-use activities and possesses very low concentrations of ions (such as nitrate) that are typically associated with agriculture. This suggests water chemistry is highly influenced in the northern part of the study area than the southern part and is least affected in the S2, S3, S6 and S8 springs. S2, S3 and S8 emerge through small conduits and S6 represents the epikarst flow of the aquifer (Dar et al. 2014b).

This understanding of aquifer heterogeneity is further validated here by the spatial variability of data. Water levels are close to the surface in the northern (group 1) samples (average 6.5 m bgl) and are 0.6 times deeper (average 10.5 m bgl) in group 2 samples (Fig. 4a). High temperatures in group 1 and 2 samples are associated with agriculture (evaporated irrigation return flow from paddy fields) and possible evaporation from near-surface groundwater. The water temperature is 0.9 times more in southern samples than elsewhere, possibly due to the large density of population and large number of tourist visits to the Belum caves. This is also observed by comparatively less alkaline conditions (pH 7.01) in group 2, followed by group 1 (average 7.15) and alkaline freshwater zone group

Table 7 Major processes operating in the karst area that either control or influence the concentration of various elements in the groundwater of the aquifer

Process operating in the area	Elemental concentrations affected
Dissolution of carbonates	Mn, Al, Se, Ba, Co, Li, Rb, Zn, V, Fe, Cd, Pb, As, Si, Cu
Weathering of quartzite and shale	Sr, Al, Li, Ag, Si
Agriculture (fertilizers/manures, organic matter)	Se, Sr, Cd, Zn, Mo, Pb, As, Cu, Cr
Industrial practices	Co, Zn, V, Fe, Ni, Cd, Ag, Pb
Urbanization/land-use changes	Se, V, Cd, Ni, Zn, Sb, Mo, Cu, Cr

Fig. 4 a Scatter plot of water level of the 17 samples shows marked variability. **b** Scatter plot of specific conductance of groundwater measured in 17 samples of the study area
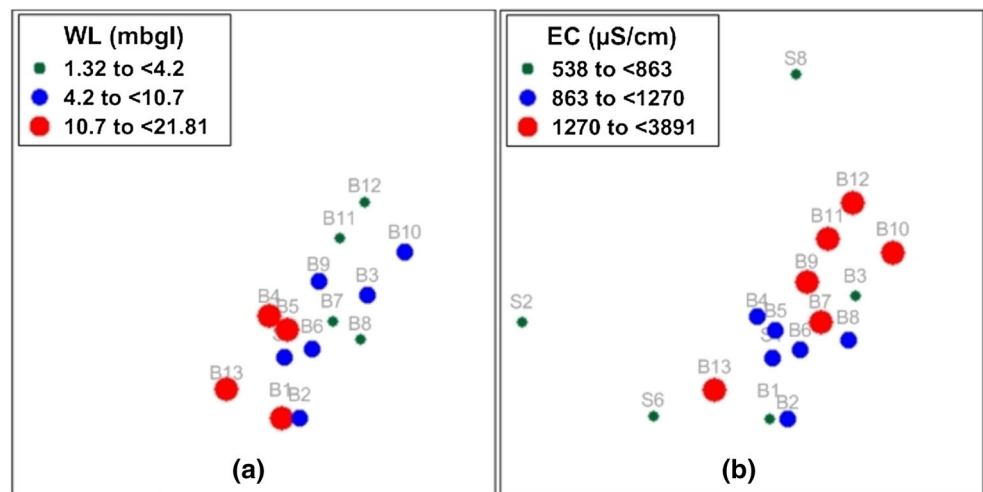
3 (S2, S6 and S8). In redox reactions, acidic conditions normally enhance the release and mobility of several elements from aquifer minerals (Vanderzalm et al. 2011; Levins and Gosk 2008) particularly in agricultural areas (Gonneea et al. 2014). This is observed in group 1 samples in the study area with comparatively lower pH and generally elevated concentrations of most of the elements. Figure 4b shows that mean EC in group 1 (2122μS/cm) is much higher than group 2 (less by factor of 2.3) and group 3 (less by factor of 3.3). Higher EC values are probably due to anthropogenic activities, fertilizer/manure applications and decomposition of organic matter. Very low EC values in S2, S6 and S8 also indicates little influence from human activities. Total hardness is also highest in group 1 (mean 397 mg/l) followed by group 2 (mean 320 mg/l) and group 3 (mean 287 mg/l). Similar behavior is shown by major ions (Ca^{2+}, Mg^{2+}, HCO_3^-, Na^+, K^+, Cl^-, F, Br, nitrate and sulfate) with comparatively higher concentrations in group 1 samples. Group 1 has a phosphate value of 1.6 mg/l in the water. The Stiff diagrams (Hem, 1985) also showed clear differences in the major ion chemical composition of the samples from the three groups. Group 1 samples have a large range (0–18 meq/l for cations and 0–12 meq/l for anions) as seen in the horizontal axis of diagram (Fig. 5), followed by smaller range in group 2 (0–6 meq/l for cations and 0–10 meq/l for anions) and even smaller range in group 3 (0-meq/l for both cations and anions). The mean elemental concentrations in the groundwater also show similar characteristics in three groups (Table 8). Except for Ca, Mn, Zn, Ag, Cd, Sb, Ba and Pb, which are highest in group 2, all other major and trace elements are higher in group 1 samples with little variation in their means. The group 1 samples have 2 times higher concentrations than group 2 and 2.7 times higher values than group 3 samples. Out of the alkaline earth metals, Ca and Ba show almost similar distribution while as Mg and Sr behave similarly.

Only Cd and Ba are highest in group 3 samples (S2 and S4) which may be associated with the enhanced dissolution of carbonate minerals in higher units of limestone.

Thus, the chemical composition of groundwater in the group 3 samples is possibly dominated by natural processes (i.e., rock weathering and dissolution) while water quality in the group 1 samples is influenced by evaporation, agriculture, fertilizers/agrochemicals and other human-related activities with an uncertain contribution from natural dissolution. Group 2 samples have mixed behavior and are more likely to be controlled by several factors such as variations in lithological characteristics (aquifer and aquitard), relative rates of weathering/dissolution of minerals, human-induced contamination, fertilizer spreading, mining activities, road tar and industries as the area has high density of population. Furthermore, in shallower water level areas, water chemistry is influenced to a larger extent by anthropogenic sources where the roles of redox reactions, pH, organic matter, fertilizers, sewage, etc. are more active.

In semiarid areas, a large volume of irrigated water from rice fields evaporates (Simpson et al. 1992; Clark and Fritz 1997) increasing the concentrations of chemical constituents in the remaining water. Based on experimental results using Cl^- and isotopes in India (Marechal et al. 2006; Negrel et al. 2011), their concentration is observed to increase 4–11 times or by an average factor of 6. Using similar approach and considering these factors the effect of evaporation on water chemistry was quantified using the chloride concentrations of groundwater as the ion behaves conservatively. The lowest Cl^- concentration in the groundwater is 13 and 17 mg/l corresponding to S2 and S3 samples of group 3. Except S6 with 175 mg/l, the average Cl^- of all the springs of the group is 32 mg/l which is even lower than the minimum concentration found in other samples. Furthermore, considering the evaporation effect
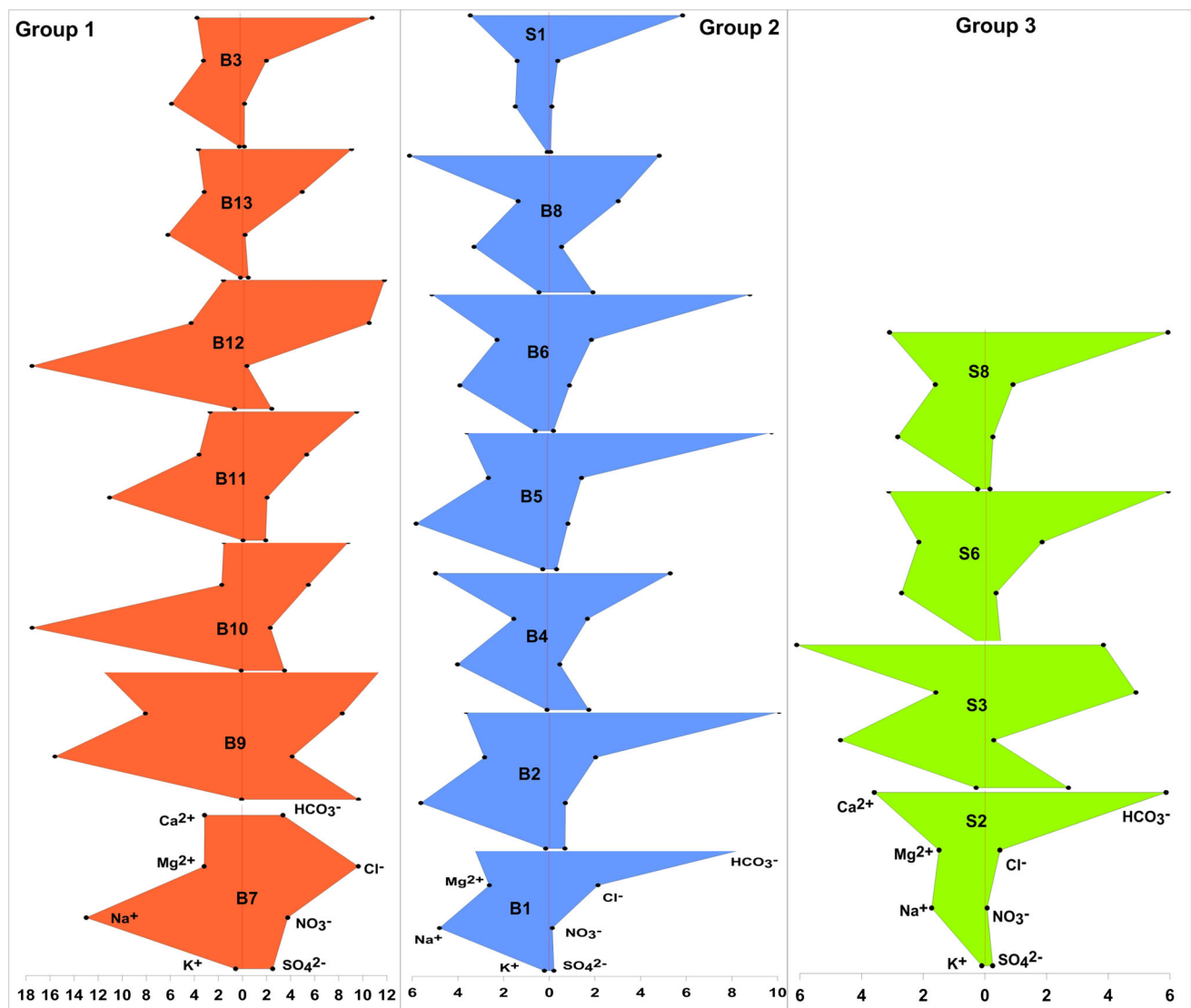
Fig. 5 Stiff diagrams showing the variability in the concentration of major ions of groundwater of three groups of samples located in Fig. 1

on rainwater Cl^-, its maximum concentration could reach 5 mg/l (weighted mean $Cl^- \approx 0.75$ mg/l multiplied by an enrichment factor of 6). After recharge occurs, rain Cl^- concentration of 5 mg/l is too low to account for the groundwater Cl of 32 mg/l that was observed in this group of samples which shows that Cl^- is mainly derived from mineral weathering with a negligible input from anthropogenic sources.

As previously discussed, groundwater from the northern part of the study area (group 1) is extensively pumped for irrigation where it is affected by evaporation and mixes with irrigation return water which increases the concentration of dissolved chemical constituents. The average concentration of Cl^- in groundwater in this area is 234 mg/l. If group 3 samples are considered to represent groundwater that has not been affected by these processes (with an

average chloride concentration of 32 mg/l), then applying a concentration factor of 6 to this water would increase the chloride concentration to 196 mg/l or about 84% of the observed average Cl^- level in the northern part of the area. Within the possible range of errors, the two average concentrations (viz. 234 and 196 mg/l) are same. However, the actual concentrations of Cl^- in group 1 samples are far higher than 234 mg/l (B3 = 76, B7 = 341.5, B9 = 294.5, B10 = 194.4, B11 = 185.5, B12 = 368.2, B13 = 174.5 mg/l). This shows the significant role of evaporation on groundwater chemistry in the area. The remaining 37.4 mg/l or 16% of Cl^- amount is likely to be associated with the application of fertilizers/manures, agrochemicals, organic matter and plant and animal waste, etc. in this group. The evaporative enrichment of groundwater during recharge is also a common process in arid and

Table 8 Mean and standard deviation of groundwater major and trace elements of three spatially distinct areas of the study area

	Group 1	Group 2	Group 3
F	1.49 ± 0.51	0.78 ± 0.17	0.79 ± 0.30
Br	1.90 ± 1.05	0.52 ± 0.34	1.63 ± 1.78
Li	0.08 ± 0.02	0.04 ± 0.005	0.01 ± 0.003
P	1.60 ± 0.71	NA	NA
Al	77.69 ± 71.10	43.32 ± 82.13	14.73 ± 4.01
Si	5.41 ± 2.40	4.21 ± 0.67	3.39 ± 0.47
V	2.83 ± 3.46	0.92 ± 0.36	0.55 ± 0.03
Cr	12.57 ± 0.51	12.54 ± 0.42	12.46 ± 0.24
Mn	6.27 ± 9.37	17.20 ± 41.01	5.23 ± 5.28
Fe	138.96 ± 105.96	76.44 ± 58.49	43.14 ± 6.67
Ni	1.25 ± 1.01	1.26 ± 0.69	1.11 ± 0.24
Co	0.11 ± 0.08	0.11 ± 0.14	0.06 ± 0.03
Cu	2.95 ± 1.76	2.41 ± 1.42	1.27 ± 0.74
Zn	62.39 ± 57.54	100.43 ± 127.5	14.40 ± 12.35
As	0.42 ± 0.40	0.16 ± 0.03	0.12 ± 0.03
Se	1.64 ± 1.25	0.77 ± 0.31	0.36 ± 0.17
Rb	0.78 ± 1.32	0.21 ± 0.18	0.31 ± 0.34
Sr	225.64 ± 198.13	77.36 ± 14.47	40.82 ± 7.72
Mo	0.55 ± 0.34	0.23 ± 0.11	0.27 ± 0.15
Ag	0.01 ± 0.003	0.005 ± 0.002	0.01 ± 0.004
Cd	0.03 ± 0.02	0.04 ± 0.08	0.04 ± 0.02
Sb	0.03 ± 0.01	0.02 ± 0.01	0.03 ± 0.02
Ba	9.27 ± 5.58	21.86 ± 12.71	41.89 ± 23.37
Pb	1.20 ± 0.56	3.17 ± 5.15	0.82 ± 0.11

semiarid regions which has been observed in many parts of the world (e.g., Sami 1992 in South Africa, Navada et al. 1999 in Rajasthan, Negrel et al. 2011 in southern India). It is likely that this process is taking place to a greater extent in parts of the study area that are receiving diffuse recharge (i.e., group 1 samples) than in areas where recharge takes place through karst conduits (i.e., group 2 samples). This evaporation effect is also observed by a slope of 4 in δ^2H–δ^{18}O relationship of the groundwater (Dar 2014) and also by Mathieu and Bariac (1996).

Groundwater quality

The study of major and trace elements in groundwater is important in relation to the health concerns associated with their increased concentration in drinking water and food (WHO 1996). The water chemistry data show that concentrations of most chemical constituents with potential health concerns are generally very low with the exception of Al which exceeds 200 µg/l (Table 3). With the exception of TDS, Na^+, NO_3^- and F, most physicochemical parameters are also below WHO (2011) recommended

limits for drinking water (Table 5). However, high variability of certain metals such as Ba, Li, Rb, Co, Na, Zn, V, Sr, Fe, Ni, Sb and Ag suggests that the role of anthropogenic and industrial contamination is increasing in the study area which is also observed by other studies as found by higher levels of certain chemicals in Table 4.

In order to appraise the level of contamination for each element, pollution indices (as percentages) were calculated by dividing the average value of element by the WHO guideline value for drinking water. Table 5 shows that Na has highest values of the pollution index (i.e., 81.6%) followed by F (70.5%), NO_3^- (60.6%) and TDS (48.8%) as they are found above in comparison with the WHO recommended levels in some samples. F levels above 1.5 mg/l in the area are of health concern as concentrations of this magnitude are known to have caused fatal fluorosis in many parts of India. The pollution index of TH is also high which together indicates the level of contamination with respect to carbonates (Ca and Mg elements). The pollution index of metals (Table 3) decreases in the order: Fe > Al > Cr > Cl > Pb > SO_4^{2-} > Ba > Se > As > Ni > Zn > Mn > Cd > Mo > Sb > Co > Cu > V > Ag. Out of these metals, Ag and Pb are considered as more toxic, Fe, Cr, As, Ni, Cd, Zn, Mn, Sb, Co, Cu, V as intermediately toxic and Li, Na, K, Ca, Mg, Al, Ba, Sr as least toxic to biological system (Adriano 2001).

Although groundwater of the aquifer is suitable for drinking and other uses, it is reasonable to conclude that anthropogenic and industrial contamination is rising to an extent that might render the water unsuitable for future uses when the vulnerable nature of karst to contamination and unmanaged land-use practices in the area are considered. A number of other issues on water quality are likely to emerge due to rise in population, urbanization, application of higher doses of fertilizers and agrochemicals, industrialization and generation of rock waste from cement plants. It is observed that cement processing plants are potentially significant sources of Al, Ca, Fe, Mg, Zn, Cu, Mn, Pb, Ti, Cd, Cr, Si and V contamination in groundwater (Lioy et al. 2009; Adejumo et al. 1994). In addition, the metal concentrations demand further detailed studies as their dietary intakes vary with different age groups. For example, a limit of 10 µg/day of Se is recommended for infants of 1 year age and 75 µg/day for lactating women (Food and Nutrition Board 1989).

Conclusion

The paper discussed the trace element concentrations of groundwater in association with major ions in the Narji Limestone aquifer of Andhra Pradesh, India, to evaluate the origin and contributing factors of elements and their

level of pollution in the aquifer. The limestone is constituted dominantly of calcite with small amounts of dolomite, silica, clay and disseminated pyrite. Trace metals are present in small amounts in the rock minerals.

It is observed that three dominant processes control the chemical composition of groundwater in the limestone aquifer. Firstly, the dissolution of carbonate minerals is the major source of elements such as Ca, Mg, Mn, Al, Cd, Ba, Sr, Co, Li, Rb, V, Fe, Pb, As, Si and Cu in groundwater. Minor quantities of several elements such as Na, K, Cl, Si and F are also likely released from minerals of quartzite and shale formations. Natural dissolution of minerals is influenced by local pH–Eh conditions, residence time and recharge mechanisms.

The values of a number of metals in groundwater including Cd, As, Cu, Pb, Zn, Mn, Sr, Cl, Br, Sb, Ag, Mo and Cu are selectively concentrated by anthropogenic processes, agricultural activities and the decay of organic matter. Intensive agricultural activities are disrupting the natural hydrogeochemical processes in the aquifer. Plant nutrients, fertilizers, manures and animal/human wastes release various inorganic chemicals into the groundwater. Significant contribution is from anthropogenic sources particularly for Na^+, K^+, Cl^-, NO_3^-, SO_4^{2-}. The presence of higher concentration of metals such as aluminum, cadmium, copper, lead, nickel, zinc, manganese, iron, cobalt, silver in agricultural areas indicates their solubility, mobility and distribution principally affected by pH and interaction with organic matter. Spatially, groundwater from the northern parts of the area shows high evaporative enrichment (about 84% increase in concentrations) and anthropogenic contamination due to fertilizers/manures, agrochemicals, plant and animal waste.

Urbanization, land-use change, mining and industrial activity increase the concentration of elements such as Cd, Se, Ni, Zn, V, Fe, Cd, Sb, Ag and Cr in groundwater. Industries operating in the area underlain by the limestone aquifer produce noticeable quantities of various major and trace elements in wastes which are causing the deterioration of groundwater quality. About 46% of samples show the effects of evaporation, agriculture and human sources of contamination of groundwater quality, whereas 29% of the samples show the influence of dissolution of aquifer minerals, agriculture and industrial contamination of groundwater quality. Groundwater in the southern part of the study area appears to be affected by sewage and waste disposal, and mining and quarrying activities.

The concentrations of various elements in groundwater are currently within the WHO recommended limits for drinking water. However, there is some evidence that the concentrations of many metals in groundwater are increasing. The decreasing order of pollution is: Fe > Al > Cr > Cl > Pb > Ba > Se > As > Ni > Cd >

Zn > Mn > Mo > Sb > Co > Cu > V>Ag. Na has highest pollution index followed by F and NO_3^- as they are found above the WHO recommended levels in some samples. A number of unmonitored and unmanaged human activities in the karst area are likely to increase the concentrations of chemicals in the groundwater and therefore demands proper management so that the aquifer remains a safe source of drinking and domestic water for the dependent population of the area.

References

Adejumo JA, Obioh IB, Ogunsola OJ, Akeredolu FA, Olaniyi HB, Asubiojo OI, Oluwole AF, Akanle OA, Spyrou NM (1994) The atmospheric deposition of major, minor and trace elements within and around three cement factories. J Radioanal Nucl Chem 179(2):195–204

Adriano DC (2001) Trace elements in terrestrial environments biogeochemistry, bioavailability, and risks of metals. Springer, New York, p 865. ISBN 978-1-4684-9505-8

Banner JL, Musgrove M, Capo RC (1994) Tracing ground-water evolution in a limestone aquifer using Sr isotopes: effects of multiple sources of dissolved ions and mineral solution reactions. Geology 22:687–690

Barbieri M, Morotti M (2003) Hydrogeochemistry and strontium isotopes of spring and mineral waters from Monte Vulture volcano, Italy. Appl Geochem 18:117–125

Berti WR, Jacobs LW (1998) Distribution of trace elements in soil from repeated sewage sludge applications. J Environ Qual 27:1280–1286

Bertram CN (2010) Sedimentology, age and stable isotope evolution of the Kurnool Group, Cuddapah basin. Masters Dissertation, the University of Adelaide. https://digital.library.adelaide.edu.au/dspace/bitstream/2440/.../2/02wholeGeoHon.pdf

Bhaskar (2009) Cement grade Limestone area in Kadapa dist. AP. A Brief note on the salient features of the cement grade limestone deposits along with concession (Lease) particulars held by Midwest granite ltd. In Cuddapah district Andhra Pradesh, south India. Midwest Granite (P) Ltd. www.scribd.com

Bicalho CC, Batiot-Guilhe C, Seidel JL, Van Exter S, Jourde H (2012) Geochemical evidence of water source characterization and hydrodynamic responses in a karst aquifer. J Hydrol 450–451:206–218

Bolland MDA, Glencross RN, Gilkes RJ, Kumar V (2005) Agronomic effectiveness of partially acidulated rock phosphate and fused calciummagnesium phosphate compared with superphosphate. Nutr Cycl Agroecosyst 32:169–183

Breit GN, Wanty RB (1991) Vanadium accumulation in carbonate rocks: a review of geochemical control during deposition and diagenesis. Chem Geol 91:83–97

Brown JG, Glynn PD (2003) Kinetic dissolution of carbonates and Mn oxides in acidic water: measurement of insitu field rates and reactive transport modeling. Appl Geochem 18:1225–1239

CGWB (2011) Groundwater information system. Central groundwater board. Ministry of water resources, Govt of India. Groundwater level and quality data is available free of cost at http://gis2.nic.in/cgwb/Gemsdata.aspx. Data Assessed on 06 May 2014

Chai LY, Wang ZY, Wang YY et al (2010) Ingestion risks of metals in groundwater based on TIN model and dose-response assessment-a case study in the Xiangjiang watershed, central-south China. Sci Total Environ 408:3118–3124

Chengxiang X, Daohong L, Zizhong L (2012) Bioaccumulation of eight heavy metals in cave animals from Dashui and Malang caves, Guizhou Province, China. Afr J Biotechnol 11(92):15931–15935

Clark I, Fritz P (1997) Environmental isotopes in hydrogeology. Lewis Publishers, Boca Raton, p 328

Cloutier V, Lefebvre R, Therrien R, Savard MM (2008) Multivariate statistical analysis of geochemical data as indicative of the hydrogeochemical evolution of groundwater in a sedimentary rock aquifer system. J Hydrol 353:294–313

Crites RW (1985) Micropollutant removal in rapid infiltration. In: Takashi A (ed) Artificial recharge of groundwater. Butterworth Publishers, Boston, pp 579–608

Dar (2014) Hydrogeological Characteristics of Carbonate Formations of the Cuddapah Basin, India. Unpublished Ph. D. thesis, University of Hyderabad, 2014, p 272

Dar FA, Perrin J, Riotte J, Gebauer HD, Narayana AC, Ahmed S (2011) Karstification in the Cuddapah Sedimentary Basin, Southern India. Implications for groundwater resources. Acta Carsologica 40(3):457–472

Dar FA, Perrin J, Ahmed S, Narayana AC (2014a) Review: carbonate aquifers and future perspectives of Karst hydrogeology in India. Hydrogeology 22(7):1493–1506. doi:10.1007/s10040-014-1151-z

Dar FA, Perrin J, Ahmed S, Narayana AC, Riotte J (2014b) Hydrogeochemical characteristics of Karst Aquifer from a semi-arid region of Southern India and impact of rainfall recharge on groundwater chemistry. Arab J Geosci 8(5):2739–2750. doi:10.1007/s12517-014-1440-9

Dar FA, Rangarajan R, Muralidharan D, Ahmed S (2015) Recharge rate in a carbonate rock covered watershed in Kurnool district, Andhra Pradesh, India using Tritium injection and Soil Water Balance methods. J Ind Geophys Union 19(4):401–413

Deng CB, Zhang CL, Li LH, Li ZY, Li N (2011) Mercury contamination and its potential health effects in a lead–zinc mining area in the karst region of Guangxi, China. Appl Geochem 26:154–159

Deverel SL, Fujii R (1988) Processes affecting the distribution of selenium in shallow ground water of agricultural areas, western San Joaquin Valley Calif. Water Resour Res 24:516–524

Deverel SJ, Goldberg S, Fujii R (2012) Chemistry of trace elements in soils and groundwater. In: Wallender WW, Tanji KK (eds) ASCE Manual and Reports on Engineering Practice No. 71 Agricultural Salinity Assessment and Management, Chapter 4, 2nd edn. ASCE, Reston, VA, pp 89–137

Dhana Raju R, Roy M, Roy M, Vasudeva SG (1993) Uranium mineralisation in the south western part of Cuddapah basin: a petromineralogical and geochemical study. J Geol Soc India 42:135–149

Dutt NVBS (1962) Geology of Kurnool System of rocks in Cuddapah and the Southern part of Kurnool District. Rec Geol Surv India 87:549–694

Farmaki EG, Thomaidis NS (2008) Current status of the metal pollution of the environment of Greece-a review. Glob NEST J 10:366–375

Fels JB (1999) Source-identification investigations of petroleum contaminated groundwater in the Missouri Ozarks. Eng Geol 52:3–13

Food and Nutrition Board (1989) Recommended dietary allowances. National Research Council, Washington

Gascoyne M (1983) Trace-element partition coefficients in the calcite-water system and their paleoclimatic significance in cave studies. In: Back W, LaMoreaux PE (Guest-Editors), V.T. Stringfield Symposium–Processes in Karst Hydrology. J Hydrol 61:213–222

Gonneea ME, Charette MA, Liu Q, Herrera-Silveira JA, Morales-Ojeda SM (2014) Trace element geochemistry of groundwater in a karst subterranean estuary (Yucatan Peninsula, Mexico). Geochim Cosmochim Acta 132:31–49

Griffith EM, Paytan A (2012) Barite in the ocean–occurrence, geochemistry and palaeoceanographic applications. Sedimentology 1 59(6):1817–1835

Guo P, Xie ZL, Li J, Zhou LF (2005) Specificity of heavy metal pollution and the ecological hazard in urban soils of Changchun City. Sci Geogr Sin 25(1):108–112

Hem (1985) Study and interpretation of the chemical characteristics of natural water. US Geological Survey Water Supply Paper 2254, US Geological Survey, Washington

Hooftman N, Oliveira L, Messagie M, Coosemans T, Mierlo JV (2016) Environmental analysis of Petrol, diesel and electric passenger cars in a Belgian Urban setting. Energies 9:84

Hu H (2002) Human health and heavy metals exposure. Chapter 4. In: McCally M (ed) Life support: the environment and human health. MIT Press, Cambridge

IARC (1990) Nickel and nickel compounds. In: Chromium, nickel and welding. IARC monographs on the evaluation of carcinogenic risks to humans, vol 49. International Agency for Research on Cancer, Lyon, pp 257–445

Jarrell WM, Page AL, Elseewi AA (1980) Molybdenum in the environment. Residue Rev 74:1–43

Jeyagopal AV, Singh RV, Rao PN, Saxena VP, Sinha RM (2006) Geology of the Julakallu Area, Palnad Sub-Basin, Cuddapah Basin, Guntur District, Andhra Pradesh. J Geol Soc India 68:103–114

Kamal MY (1974) Sedimentology and sedimentary tectonics of the Kurnool system, near Kurnool. Unpublished thesis, Osmania University, Hyderabad

Kilroy G, Coxon C (2004) Temporal variability of phosphorus fractions in Irish karst springs. Environ Geol 47:421–430

Kumar JV (1983) Geological and hydrogeological studies of part of Cuddapah basin. Ph. D. thesis. Osmania University, Hyderabad

Langmuir D (1978) Uranium solution-mineral equilibria at low temperatures with applications to sedimentary ore-deposits. Geochim Cosmochim Acta 42(6):547–569

Leung CM, Jiao JJ (2006) Heavy metal and trace element distributions in groundwater in natural slopes and highly urbanized spaces in Mid-Levels area, Hong Kong. Water Res 40:753–767

Levins I, Gosk E (2008) Trace elements in groundwater as indicators of anthropogenic impact. Environ Geol 55:285–290

Li XD, Liu CQ, Harue M, Li SL, Liu XL (2010) The use of environmental isotopic (C, Sr, S) and hydrochemical tracers to characterize anthropogenic effects on karst groundwater quality: a case study of the Shuicheng Basin, SW China. Appl Geochem 25:1924–1936

Li J, Li FD, Liu Q et al (2014) Impacts of Yellow River irrigation practice on trace metals in surface water: a case study of the Henan-Liaocheng irrigation area, China. Hum Ecol Risk Assess 20:1042–1057

Lioy PJ, Fan ZH, Yu CH (2009) Final Report: Contribution of Particle Emissions from a Cement-Related Facility to Outdoor Dust in Surrounding Community. UMDNJ-Robert Wood Johnson

Medical School and Environmental and Occupational Health Sciences Institute 170 Frelinghuysen Road Piscataway, NJ 08854. http://www.state.nj.us/dep/dsr/cement-study/final-outdoor-dust.pdf. Downloaded on 11-03-2017

Long DT, Voice TC, Niagolova ND, McElmurry SP (2012) Effects of human activities on karst groundwater geochemistry in a rural area in the Balkans. Appl Geochem 27:1920–1931

Marechal JC, Dewandel B, Ahmed S, Galeazzi L, Zaidi FK (2006) Combined estimation of specific yield and natural recharge in a semi-arid groundwater basin with irrigated agriculture. J Hydrol 329:281–293

Markovic T, Miko S, Kapelj Buljan R, Larva O, Peh Z (2006) Behaviour of metals and nutrients in soils and groundwater of a karst polje. J Geochem Explor 88:124–129

Mathieu R, Bariac T (1996) An isotopic study (2H and 18O) of water movements in clayey soils under a semiarid climate. Water Resour Res 32:779–789

Mattigod SV, Page AL (1983) Assessment of metal pollution in soils. In: Thornton I (ed) Applied environmental geochemistry. Academic Press, London, pp 355–391

Morse JW, Mackenzie FT (1990) Geochemistry of sedimentary carbonates. Elsevier, Amsterdam, p 706

Mouli AC, Hanumanthu RC, Rao RJ (2012) Conflicting land-use practices in the Narji Limestone Belt in YSR District, Andhra Pradesh (AP), India. J Earth Sci India, Popular Issue III:1–9. www.earthscienceindia.info

MSME-Development Institute (2011) Brief industrial profile of Kurnool District. Ministry of MSME, Govt. of India, Hyderabad. http://dcmsme.gov.in/dips/Kurnool%20dip%20%20amended%20march.pdf. Website Accessed on 10 Aug 2015

Navada SV, Nair AR, Sinha UK, Kulkarni UP, Joseph TB (1999) Application of isotopes and chemistry in unsaturated zone in arid areas of Rajasthan, India. TecDoc IAEA 1246:119–130

Negrel P, Pauwels H, Dewandel B, Gandolfi JM, Mascre C, Ahmed S (2011) Understanding groundwater systems and their functioning through the study of stable water isotopes in a hard-rock aquifer (Maheshwaram watershed, India). J Hydrol 397:55–70

Patranabis-Deb S, Saha D, Tripathy V (2012) Basin stratigraphy, sea-level fluctuations and their global tectonic connections—evidence from the Proterozoic Cuddapah Basin. Geol J 47(2–3):263–283

Peryea FJ, Creger TL (1994) Vertical distribution of lead and arsenic in soil contaminated with lead arsenate pesticide residues. Water Air Soil Pollut 78:297–306

Purushotham D, Rashid M, Lone MA, Rao AN, Ahmed S, Nagaiah E, Dar FA (2013) Environmental impact assessment of air and heavy metal concentration in groundwater of Maheshwaram watershed, Ranga Reddy District, A. P, India. J Geol Soc India 81:385–396

Radell MJ, Katz BG (1991) Major-ion and selected trace-metal chemistry of the Biscayne aquifer, Southeast Florida. U. S. Geological Survey, Water-resources investigations report, Reston, pp 91–4009

Rafi KM, Ramachar T, Umamahesh M (2012) The chemical investigation on water pollution of Kurnool district by water quality analysis. Online J Sci Technol 2(1):1–9

Rai AK, Zakaulla S, Vidyasagar D, Murgan MG, Birua MK, Sivasubramanian R (2011) Geochemistry of the uraniferous dolostones from areas around Kanampalle in south western margin of Cuddapah Basin. Indian Minerol 45(1):24–35

Rao PB, Subrahmanyam K, Dhar RL (2001) Geoenvironmental effects of groundwater regime in Andhra Pradesh, India. Environ Geol 40(4–5):632–642

Rao DS, Vijayakumar TV, Prabhakar S, Bhaskar Raju G (2011) Geochemical assessment of a siliceous limestone sample for cement making. Chin J Geochem 30:33–39

Saha D, Tripathy V (2012) Tuff beds in Kurnool subbasin, southern India and implications for felsic volcanism in Proterozoic intracratonic basins. Geosci Front 3(4):429–444

Sami K (1992) Recharge mechanisms and geochemical processes in a semi-arid sedimentary basin, Eastern Cape, South Africa. J Hydrol 139:27–48

Sarkar A, Chakraborty PP, Mishra B, Bera MK, Sanyal P, Paul S (2010) Mesoproterozoic sulphidic ocean, delayed oxygenation and evolution of early life: sulphur isotope clues from Indian Proterozoic basins. Geol Mag 147(2):206–218. doi:10.1017/S0016756809990380

Sengupta SM (2007) Introduction to sedimentology, 2nd edn. CBS Publishers, New Delhi, p 339. ISBN 81-239-1491-1

Shapiro SS, Wilk MB (1965) An analysis of variance test for normality. Biometrika 52(3–4):591–611. doi:10.1093/biomet/52.3-4.591.JSTOR2333709

Simpson HJ, Herczeg AL, Meyer WS (1992) Stable isotope ratios in irrigation water can estimate rice crop evaporation. Geophys Res Lett 19:377–380

Singh RV, Sinha RM, Bisht BS, Banerjee DC (2002) Hydrogeochemical exploration for unconformity-related uranium mineralization: example from Palnadu sub-basin, Cuddapah Basin, Andhra Pradesh, India. J Geochem Explor 76:71–92

Statistical Abstracts (1966–97) Directorate of Economics and Statistics, Government of Andhra Pradesh, Hyderabad, India

Sunitha V, Reddy BM, Reddy MR (2014) Mineral resources of Cuddapah Basin. J Biol Chem Res 31(1):226–235. ISSN 0970-4973 (Print) ISSN 2319-3077

Underwood E (2012) Trace elements in human and animal nutrition. Elsevier, Amsterdam, p 442

USEPA (1989) Ground-water monitoring in Karst Terranes-recommended protocols & implicit assumptions. (EPA/600/X-89/50):88. http://www.epa.gov/oust/cat/gwkarst.pdf

USEPA (2011) Drinking water standards and health advisories United States Environmental Protection Agency. EPA 820-R-11-002

Vanderzalm JL, Dillon PJ, Barry KE, Miotlinski K, Kirby JK, La Salle CLG (2011) Arsenic mobility and impact on recovered water quality during aquifer storage and recovery using reclaimed water in a carbonate aquifer. Appl Geochem 26:1946–1955

Vijayam BE, Kamal MY, Veeriah K (1981) Sedimentation in the Kurnool group. Fourth workshop on status, problems and programmes in Cuddapah basin. Indian Inst. Peninsular Geol., Hyderabad

Vittal KPR, Ali M, Chary GR, Sankar GRM, Ramakrishna YS, Srijaya T, Samra JS, Singh G (2005) District wise promising technologies for rainfed pigeon-pea based production system in India. Central Research Institute for Dryland Agriculture Santoshnagar, Hyderabad

Wang Y, Guo Q, Su C, Ma T (2006) Strontium isotope characterization and major ion geochemistry of karst water flow, Shentou, northern China. J Hydrol 328:592–603

WHO (1996) Trace elements in human nutrition and health. World Health Organization, Geneva

WHO (2006) Environmental Health Criteria. Elemental speciation in human health risk assessment. WHO Press, World Health Organization, Geneva

WHO (2011) World Health Organization (2003) Guidelines for Drinking Water Quality, 4th edn. WHO Press, World Health Organization, 20 Avenue Appia, 1211 Geneva 27, Switzerland.http://www.who.int/water_sanitation_health/dwq/guidelines/en/index.html

Wong CI, Mahler BJ, Musgrove M, Banner JL (2012) Changes in sources and storage in a karst aquifer during a transition from drought to wet conditions. J Hydrol 468–469:159–172

Yao PH, Shyu GS, Chang YF, Chou YC et al (2015) Lead isotope characterisation of petroleum fuels in Taipei, Taiwan. Int J Environ Res Public Health 12:4602–4616

Zachariah JK, Bhaskar Rao YJ, Srinivasan R, Gopalan K (1999) Pb, Sr and Nd isotope systematics of uranium mineralized stromatolitic dolomites from the Proterozoic Cuddapah Supergroup, south India: constraints on age and provenance. Chem Geol 162:49–64